

Novel Coplanar EBG Low Pass Filter

Xing-Jun Wang^{1, 2} and Ling-Feng Shi^{1, *}

Abstract—The traditional coplanar electromagnetic bandgap (EBG) structure is analyzed. The method is studied to lower the center frequency and broaden the bandwidth in this paper. A novel structure of U-bridged EBG power plane is proposed. The simulation and test results show that the bandwidth of the new structure is 4.32 GHz, and the lower side cutoff frequency is at 380 MHz with the stopband depth at -40 dB. The elimination of simultaneous switching noise (SSN) as this kind of U-bridged coplanar EBG structure is more effective below 1 GHz. In addition, the eye diagram of the structure is analyzed. The degradation of the maximum eye open and the maximum eye width on the structure is about 1.2% and 5.7%, respectively. Finally, the IR-drop and dc resistance is accurately investigated through 3-D simulations.

1. INTRODUCTION

The degradation of the signal integrity (SI) due to the simultaneous switching noise (SSN) has become a choke point to the designing and manufacturing of the high-speed digital circuit with increasing requirements of high clock frequency [1–6]. In [1], EBG (electromagnetic bandgap) surfaces suppression of the PPW noise by 53% is achieved based on time-domain reflectometry experiments, while maintaining the signal transmission quality within the required specifications for common signaling standards, using three layers structure so that increases the cost of the fabrication. In [2], a novel method of arranging EBG unit cells on both the power/ground planes in multilayer PCBs (printed circuit board) and packages is proposed, not only as a means of sufficiently suppressing the propagation of power noise, but also as a means of minimizing the effect of EBG-patterned reference planes on a high-speed signal. However, on the assumption that noise sources and noise-sensitive devices exist only in specific areas, the proposed method is limited in its universality. Literature [3] proposes a novel stopband-enhanced electromagnetic-bandgap structure to suppress the power/ground noise on a three-layer package based on the ground surface perturbation concept. However, its three-layer package leads to increasing cost to be fabricated. Literature [4] using a complementary spiral resonator mounted on the power plane, simultaneous switching noise and ground bouncing noise can be suppressed over a very wideband under a noise suppression margin of -25 dB. However, the suppression of SSN is worse than other methods. Literature [5] proposes a new method to estimate SSN directly from the power delivery network (PDN) frequency-domain impedance in order to reduce the time-domain simulation of SSN and computational burden, which is based on the periodic characteristics of the switching current and the SSN produced by one current pulse. However, the method is fit for analysis of PDN. Literature [6] proposes a compact notched ultra-wideband (UWB) bandpass filter with improved out-of-band performance using quasi EBG structure. However, the notched band is only at -10 dB worse than other depression depth at -20 dB. Therefore, many designers begin to focus on the elimination and suppression of the SSN [7–24]. Literature [7] proposes a novel L-bridged electromagnetic bandgap (EBG) power/ground plane with super-wideband suppression of the ground bounce noise (GBN) from 600 MHz to 4.6 GHz. However, the low cut-off frequency is higher than other EBG. Literature [8] presents a novel π -bridged photonic

Received 9 April 2014, Accepted 16 May 2014, Scheduled 22 August 2014

* Corresponding author: Ling-Feng Shi (lfshi@mail.xidian.edu.cn).

¹ Key Lab of High-Speed Circuit Design and EMC, Ministry of Education, Xidian University, Xi'an, Shaanxi 710071, China.

² Electronic and Information College of Shaanxi Institute of Technology, Xi'an, Shaanxi 710300, China.

bandgap (PBG) power/ground plane with ultra-broadband suppression of the ground bounce noise (GBN) in the high-speed printed circuit boards. However, the SI is not studied in [8]. In [9], a novel design of power/ground plane with planar EBG structures for SSN is presented, which is based on using meander lines to increase the effective inductance of EBG patches. However, the area of the test PCB is more than other EBG. Literature [10] proposes an embedded band selective (EBS) power plane using the hybrid-cell periodic structure, which has ultra-wideband suppression of SSN at -60 dB. However, the low cut-off frequency of the EBG is only 1 GHz. Literature [11] proposes two leafy EBG structures for UWB SSN suppression in power/ground plane pairs. However, the SI is not studied in [11]. Literature [12] presents a novel array design etching EBG structures on both the power plane and ground plane in the region of noise source and noise-sensitive devices to mitigate SSN based on the concept of localization, which obtain UWB. However, the SI is not studied, and the area of PCB is more than other EBG. Literature [13] proposes a novel UWB bandpass filter (BPF) with a notch band, in which the filter is realized by using a high-pass filter (HPF) and an array of multiband EBG cells etched on the ground of a $50\ \Omega$ microstrip line. However, the low cut-off frequency is 3.8 GHz more than other EBG. In [14], Sierpinski space-filling curves are introduced and employed to construct the unit-cell topologies of EBG structures with different bridges, which obtain UWB. However, the SI is not studied in [14]. Literature [15] proposes a novel uniplanar compact EBG structure for UWB suppression of GBN in multilayer PCB. However, the area of the test PCB is more than other EBG. Literature [16] investigates periodic ground via lattice to suppress the propagation of parallel-plate mode between two ground planes in a multiple layer package or printed circuit board, which uses a three-layer structure, thus increases the cost of the fabrication. Literature [17] presents a novel power/ground planes design for eliminating GBN in high-speed digital circuits by using low-period PBG structure, whose low cut-off frequency is 1 GHz more than other EBG. Literature [18] proposes a power plane with wideband SSN suppression using a novel multi-via EBG structure, whose low cut-off frequency is 2.8 GHz more than other EBG. Literature [19] presents a spiral-shaped power island structure that can effectively suppress SSN when the power plane drives high-speed integrated circuits in a small area, whose low cut-off frequency is about 500 MHz more than other EBG. Literature [20] covers the concept of embedding EBG structures in conventional power distribution networks in order to increase the immunity of the circuits that feed from such networks to noise and voltage fluctuations, whose low cut-off frequency is about 2 GHz more than other EBG. Literature [21] proposes a new wideband and compact bandstop filter using one dimensional (1-D) mushroom-like EBG structures, which cannot be fabricated as easily as defected ground structure (DGS) filters. Literature [22] builds a test vehicle consisting in a 12-layer printed circuit board in standard FR4 material, whose fabrication cost is more than other EBG. Literature [23] proposes a novel wideband EBG structure for EMI reduction in multilayer PCBs, whose stopband is only 1.5 GHz. Literature [24] discusses a new isolation concept using EBG structures, whose low cut-off frequency is about 700 MHz more than other EBG. The EBG structure introduced for the suppression of SSN in recent years is a kind of periodic planar structure. The SSN is distributed in a wide range of frequency from DC (Direct Current) to the highest harmonics of the switching current of interest [18], while the center frequency of the earlier EBG structure is not low enough, and the bandwidth is too narrow to cover the frequency range below 1 GHz where the SSN energy is dominant [7]. Therefore, the research of the EBG structure is focused on lower the center frequency and is broadened the bandwidth. The center frequency and bandwidth of the I-bridged coplanar EBG structure proposed in [1] is 2.4 GHz and 3 GHz, respectively, with the lower side cutoff frequency as 1 GHz, while the L-bridged coplanar EBG structure proposed in [7] provides 2.6 GHz center frequency, 4 GHz bandwidth and 600 MHz lower side cutoff frequency. Many researchers studied super-wideband [7–15] or the methods of broadening the bandwidth [16–21]. The new fruits on EBG are applied to the design of the antennas [25–27].

2. STRUCTURE DESIGN

2.1. U-Bridge EBG Structure

A novel coplanar EBG structure with a U-shaped bridge line connecting the neighboring units is designed in this paper. The unit of the proposed U-bridged coplanar EBG structure and its corresponding parameter notations are shown in Figure 1. The parameters in Figure 1 are following: $a = 30$ mm, $s = 13.6$ mm, $n = 6$ mm, $t = 0.2$ mm, $r = 1.2$ mm, $e = 15.1$ mm, and $c = 0.8$ mm.

To demonstrate the effectiveness of the U-shaped connecting line, the paper proposes a two-layer PCB where the nine-unit EBG structure designed on the power plane and the ground plane is continuous. The top view of nine units of U-bridged coplanar EBG structure is shown in Figure 2. Figure 3 is the test PCB with the same size of Figure 2 and dielectric constant of 4.4.

The dimension of the nine-unit EBG board with the EBG structure on the top plane and continuous ground on the bottom plane is $90 \times 90 \times 0.4 \text{ mm}^3$ as shown in Figure 2. The board in Figure 3, which has the same size and substrate as in Figure 2 is made PCB to test insert loss. The 0.4 mm thickness of FR4 substrate with dielectric constant of 4.4 is embedded between the top and bottom layers. As shown in Figure 3, the original point (0, 0) is set on the left corner of the board, and three test ports from 1 to 3 are located at (15 mm, 15 mm), (75 mm, 75 mm) and (15 mm, 75 mm), respectively. The HFSS of Ansoft Corporation is used to simulate the S -parameters between two ports lying across several units of the EBG structure, which is sufficient to show the frequency bandgap of the structure [3, 9, 14]. The S -parameters for the same ports of I-bridged EBG structure are introduced in [1], and the L-bridge EBG structure introduced in [7]. Moreover, the reference structures are also simulated to compare the suppression performance of SSN, in which the power and ground plane are solid.

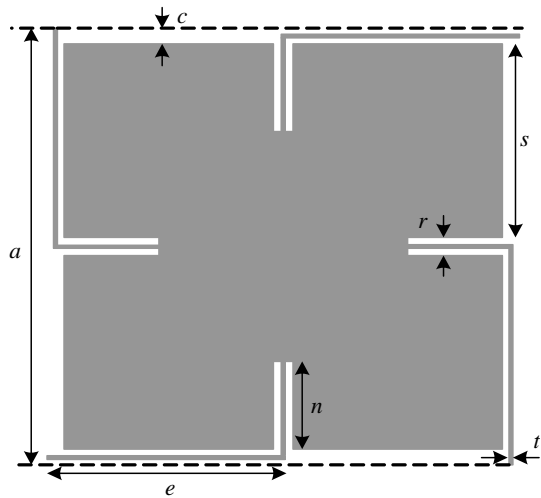


Figure 1. A unit of the U-bridged coplanar EBG structure..

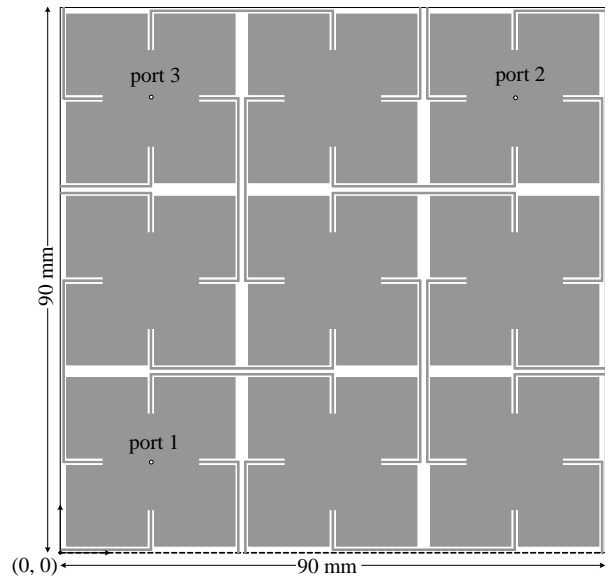


Figure 2. Top view of the nine units of the U-bridged EBG board.

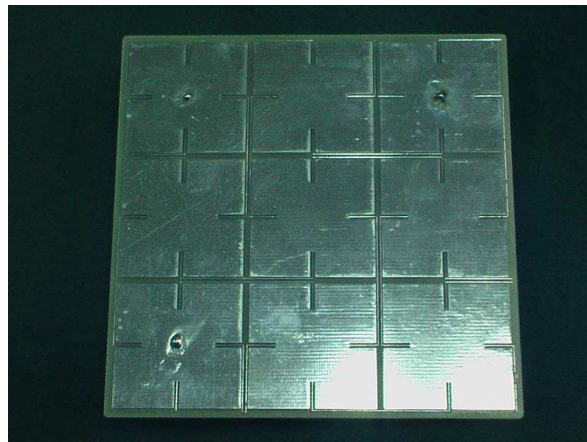


Figure 3. The fabricated test PCB on the nine units of the U-bridged EBG board.

The comparison sheet of EBG parameters is shown in Table 1.

Table 1. The compare sheet of parameters with different EBG.

Literatures	Patch area (mm ²)	Length (mm)	Thick (mm)	Number of patch
Ref. [1]	100 * 100	10	3.08	10 * 10
Ref. [2]	180 * 180	30	0.4	3 * 3
Ref. [3]	60 * 60	20	0.125 + 0.875	3 * 3
Ref. [7]	90 * 90	30	0.4	3 * 3
Ref. [8]	90 * 90	30	0.4	3 * 3
Ref. [9]	90 * 150	30	1.54	3 * 5
Ref. [10]	90 * 90	30	0.4	3 * 3
Ref. [11]	90 * 150	30	0.4	3 * 5
Ref. [13]	20 * 50	10	1.57	2 * 5
Ref. [15]	90 * 150	30	0.8	3 * 5
Ref. [17]	90 * 90	30	0.4	3 * 3
Ref. [19]	90 * 90	30	0.4	3 * 3
Proposed EBG	90 * 90	30	0.4	3 * 3

2.2. Analysis and Equivalent Model

When the wavelength is longer than the size of the individual units in these periodic EBG structures, the surface impedance can be represented by an equivalent parallel resonant LC circuit [16]. The bridge connecting the adjacent units induces the inductance L , and the gap between the two neighboring units causes the fringe capacitance C [2]. Based on the resonance characteristics of the parallel LC circuit, the impedance is infinitely great, and the SSN around the resonant frequency is eliminated from spreading over the surface of EBG structure and then flows to the return path through a low-impedance channel between the EBG structure plane and the ground plane. Therefore, the frequency bandgap centered at the resonant frequency formed by the EBG structure can suppress the transmission of the SSN. The center frequency of the bandwidth for the EBG structure can be expressed as Equation (1).

$$f_0 = \frac{1}{2\pi\sqrt{LC}} \quad (1)$$

and the bandwidth can be expressed as Equation (2).

$$BW = \frac{1}{\eta} \sqrt{\frac{L}{C}} \quad (2)$$

where η is the free space wave impedance.

In order to lower the center frequency of the EBG structure, it is necessary to increase the inductance L of the connecting line and capacitance C induced by the gap between the adjacent units based on Equation (1). However, increasing the capacitance C leads to decrease of the bandwidth according to Equation (2). Therefore, the proposed method to lower the center frequency and widen the bandwidth is to improve the inductance L [2, 8, 9].

Better to represent the EBG structures presented in literatures [1, 7], the longer connecting line and the narrower width significantly increase the effective inductance between the neighboring units. Figure 4 shows the equivalent circuit model for one unit of the U-bridged coplanar EBG structure. The propagation characteristics between the EBG patch and the continuous ground plane are represented by the inductance L_e and capacitance C_e ; the inductance of the connecting line and the capacitance induced by the gap are represented by inductance L_u and capacitance C_u . Both L_e and C_e are related with the size of the patch. Moreover, L_e is inversely proportional to the size of the patch while C_e is

proportional to the size of the patch. Both L_u and C_u are related with the size of the gap. In addition, L_u is proportional to the length of the connecting line on the gap while C_u is inversely proportional to the distance of the gap. The parameters are shown as Equations (3) to (6) [28].

$$C_e = \epsilon_0 \epsilon_r \frac{S}{h} \tag{3}$$

$$L_e = \mu_0 h \frac{len}{w} \tag{4}$$

$$L_u = len \cdot k \cdot \ln(2\pi h/w) \tag{5}$$

$$C_u = \frac{\epsilon_0(1 + \epsilon_r)l}{\pi} \cosh^{-1} \left(\frac{p}{g} \right) \tag{6}$$

where ϵ_0 and μ_0 are the permittivity and permeability of free space, respectively. ϵ_r is the relative dielectric constant, S the plane area of face to face, h the thickness of the power plane medium, len the long of transmission line, w the width of transmission line, k the constant as 0.2 nH/mm, l the side length of square EBG, p the period length of EBG, and g the gap of border upon EBG. Taking parameters in above equations, $L_e = 30.5$ nH, $C_e = 20.025$ pF, $L_u = 75.86$ nH.

The equivalent circuit model for one unit of the U-bridged coplanar EBG structure is shown in Figure 4. In low frequency, as C_u is small enough, it is ignored. Therefore, the simplified equivalent circuit model is shown in Figure 5.

The low cut-off frequency is shown in Equation (7) on parallel LC circuit in Figure 5 [29].

$$f_L = \frac{1}{\pi} \sqrt{\frac{1}{(L_e + L_u) \cdot C_e}} = 218.2 \text{ MHz} \tag{7}$$

The parallel plane resonance cavity model is used to calculate presented EBG upper cut-off frequency [20], which is the main model frequency generated by EBG power and projection ground [30]. The resonance frequency of the rectangle resonance cavity is shown as Equation (8).

$$f_{m,n} = \frac{1}{2\pi\sqrt{\mu\epsilon}} \sqrt{\left(\frac{m\pi}{a}\right)^2 + \left(\frac{n\pi}{b}\right)^2} \tag{8}$$

where μ and ϵ are permeability and permittivity of medium, respectively; m and n are wave exponent not zero; a and b are the length and width of power plane. EBG upper cut-off frequency f_H is the main model frequency. The upper cut-off frequency of the proposed U-bridge EBG is shown as Equation (9).

$$f_H = f_{1,0} = \frac{1}{2l\sqrt{\mu\epsilon}} = 5 \text{ GHz} \tag{9}$$

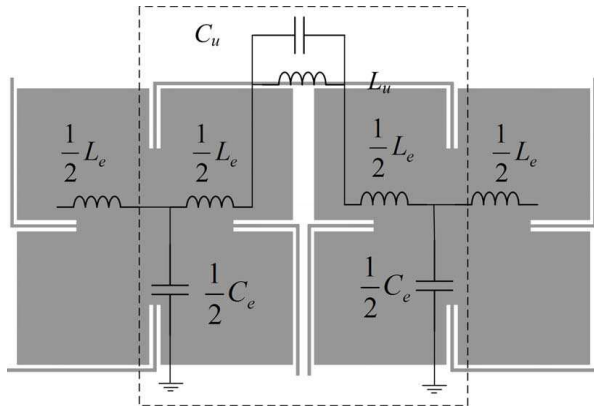


Figure 4. Equivalent circuit model for one unit of the U-bridged coplanar EBG structure.

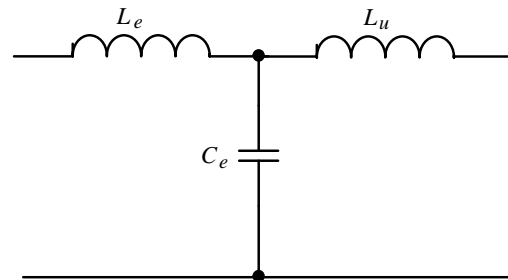


Figure 5. The simplified equivalent circuit model.

3. ANALYSIS OF THE SIMULATION AND TEST RESULTS

Figure 6 shows the simulation result $|S_{21}|$ of the U-bridged EBG board, the inserted loss of the reference board with continuous power and ground planes, the I-bridged EBG board, and the L-bridge EBG board. The compared reference board possesses the same size and substrate as U-bridged EBG board in Figure 6. The definition of bandwidth in this paper is the continuous frequency range, where the $|S_{21}|$ is maintained lower than -40 dB. It is obvious that the U-bridged EBG structure possesses a wide bandwidth of 4.32 GHz in the frequency range from 380 MHz to 4.7 GHz. The lower cut-off frequency of 380 MHz covers a large part of low frequency range below 1 GHz where the SSN energy is dominant. The 3 GHz bandwidth from 1.1 GHz to 4.1 GHz of the I-bridged EBG board for the suppression of the low frequency SSN is invalid. The comparison results of $|S_{21}|$ between the U-bridged EBG board and L-bridge EBG board presented in Figure 6 show that the U-bridged EBG structure is more efficient for elimination of the low frequency SSN than the L-bridge EBG board. Therefore, the U-bridged EBG structure is more efficient for elimination and suppression of the low frequency SSN.

Figure 7 shows the simulation results for the noise excitation at port 2 and port 3 on the U-bridged EBG board, respectively. The receiving ports are all at port 1. $|S_{21}|$ and $|S_{31}|$ are almost the same in the frequency range from DC to 6 GHz. Therefore, there is no relationship between the elimination capability of the noise and the noise excitation location.

Vector network analyzer (VNA) is used to measure the insertion loss of the U-bridged EBG PCB. The test results of PCB are shown by VNA in Figure 8 and Figure 9, respectively. The comparisons of the simulation with test show that the proposed U-bridged EBG can obtain the consistency of theory on experiment based on Figure 8 and Figure 9.

Based on Equations (7) and (9), the low cut-off frequency f_L and upper cut-off frequency f_H are 218.2 MHz and 5 GHz, respectively. The results of theory are accordant to the results of simulation with HFSS in Figure 7. It is shown that the simplified equivalent circuit model is valid.

4. SIGNAL INTEGRITY

The degradation of the U-bridged EBG structure power plane to the signal integrity is analyzed and simulated in Section 4. Figure 10 shows a four-layer PCB with the dimension of $90 \times 90 \times 1.2 \text{ mm}^3$, where the first layer and fourth layer are signal planes, the second layer U-bridged EBG structure power plane, and the third layer solid ground plane. The FR4 substrate with thickness of 4 mm and dielectric constant of 4.4 is embedded between any adjacent layers. Only a signal trace of 67 mm passing from the first layer to the fourth layer and back to the first layer with two via transitions along the path [7] is considered, as shown in Figure 10.

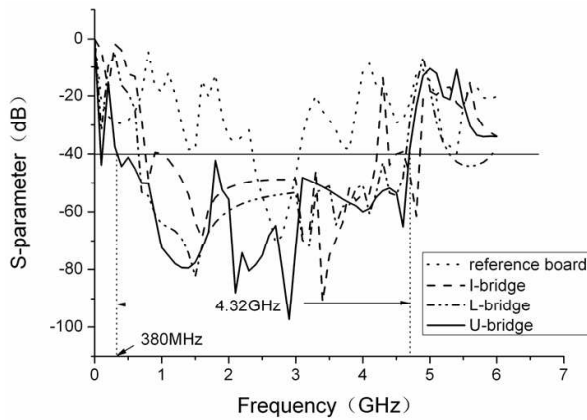


Figure 6. $|S_{21}|$ of the nine-unit U-bridged EBG board, the reference structure board, I-bridge EBG board, and L-bridge EBG board by the HFSS simulation.

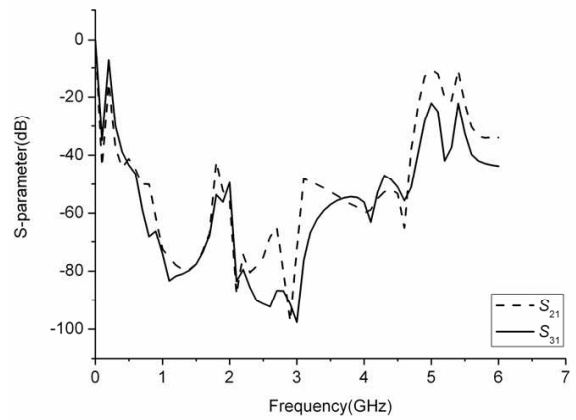


Figure 7. Comparison $|S_{21}|$ and $|S_{31}|$ located at different ports on the nine-unit U-bridged EBG board by the HFSS simulation.

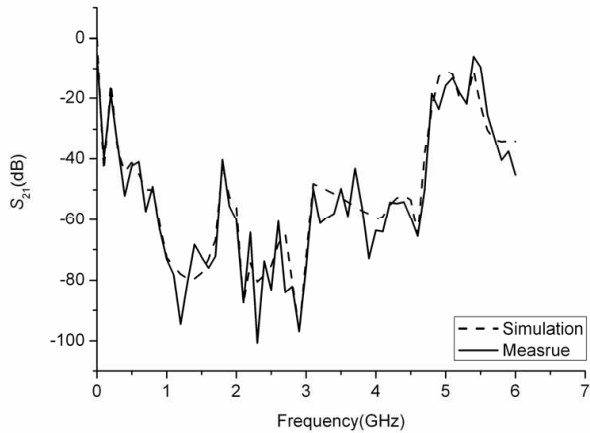


Figure 8. Comparison the HFSS simulation and test PCB on $|S_{21}|$ located between port 1 and port 2 on the nine-unit U-bridged EBG board.

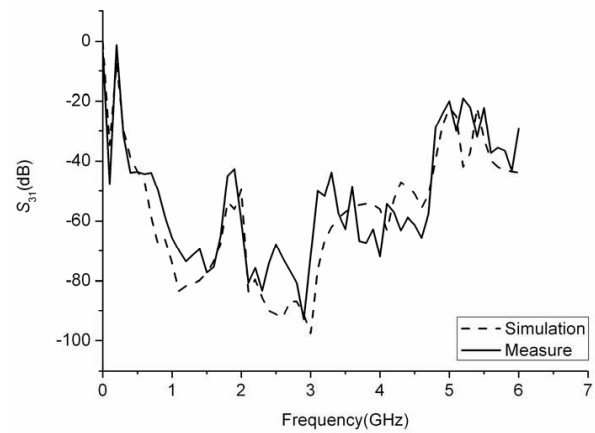


Figure 9. Comparison the HFSS simulation and test PCB on $|S_{31}|$ located between port 1 and port 3 on the nine-unit U-bridged EBG board.

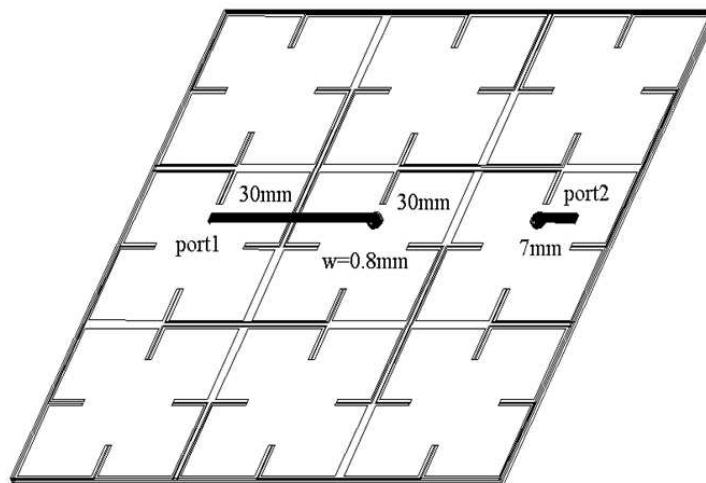


Figure 10. Four layers PCB with U-bridged EBG power plane.

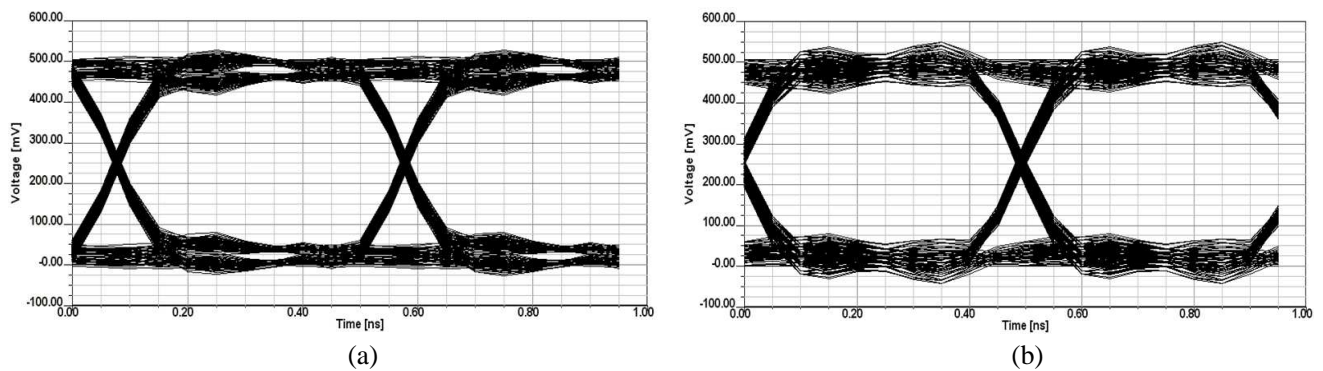


Figure 11. The eye diagram simulation. (a) The eye diagram for the reference board. (b) The eye diagram for U-bridged EBG board.

A non-return to zero (NRZ) pseudorandom binary sequence (PRBS) $2^{10} - 1$ is sent at input port 1 [7], and the eye diagram at output port 2 is simulated. The PRBS with 500 mV swing are coded at 2 GHz, and the rise or fall time is 120 ps. The maximum eye open (MEO) and maximum eye width (MEW) are used as metrics of the eye diagram quality. The eye diagram of the reference four-layer PCB with solid power plane on the second layer is shown in Figure 11(a), where MEO = 340 mV and MEW = 350 ps.

The eye diagram of the four-layer PCB with U-bridged EBG structure power plane is shown in Figure 11(b) showing MEO = 336 mV and MEW = 330 ps. The degradation of the MEO and MEW for the U-bridged EBG board is about 1.2% and 5.7%, respectively, emphasizing that the SI of the U-bridged coplanar EBG structure is acceptable.

5. IR-DROP ANALYSIS

The design of EBG needs that the voltage regulators (VRM) supply the circuits by power distribution network (PDN) at lowest cost, which means the smallest dc voltage drop during the power transport. The IR-drop is to describe the dc-drop between the VRM and the port.

The dc resistance of the proposed EBG structure is larger than the integrated power and ground plane because of its bridge. In the paper, the IR-drop of the PDN for the proposed structure is analyzed by CST EM Studio [31, 32]. The tool source and sink 1 A current flow into the ports of the power and ground plane for the proposed structure, respectively. According to simulation, the dc-drop between the current ports on the power plane (dc-drop) is obtained as shown in Figure 12. The resistance between the VRM and port can be computed according to the Ohm law. The current is 1 A, and the resistance of the whole PDN (RDC) can be expressed as Equation (10).

$$R_{DC} = \frac{(dc - drop_p + dc - drop_g)}{1 \text{ A}} = (dc - drop_p + dc - drop_g) \Omega \quad (10)$$

As shown in Figure 12(a), it can be calculated that the RDC1 of the proposed structure with U-bridge on the ground is equal to 61.3 m Ω , which will be tolerated by the PDN and voltage noise margin generally. While the RDC2 of the proposed structure with U-bridge on the ground is 73.4 m Ω in Figure 12(b), and it will result in dc-drop of 73.4 mV if the current consumption is 1 A in area. Although the U-bridge on the ground improves the noise suppression, it will lead to an IR-drop. Thus, the application of the U-bridge EBG should take the current consumption and voltage noise margin into consideration.

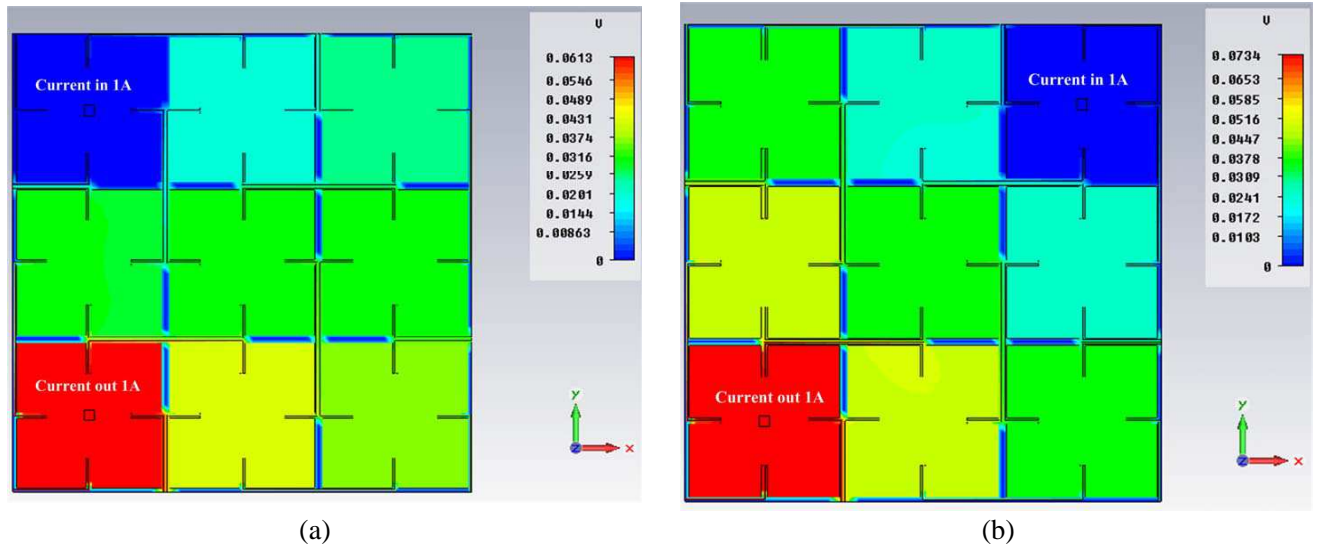


Figure 12. The IR-drop of U-bridged EBG board. (a) The IR-drop of beeline ports for U-bridged EBG board. (b) The IR-drop of diagonal ports for U-bridged EBG board.

6. CONCLUSIONS

A novel structure of U-bridged EBG power plane is proposed based on the analysis of traditional coplanar EBG structure. The method uses increased length of the connecting line with U-shaped bridge between adjacent units to obtain lower center frequency and wider bandwidth. The HFSS simulation and test results show that the bandwidth of the proposed structure is 4.32 GHz, and the low side cutoff frequency is at 380 MHz with stopband depth at -40 dB. The elimination of SSN for this kind of U-bridged coplanar EBG structure is more effective below 1 GHz. In addition, the eye diagram of the structure is analyzed. The degradation of MEO and MEW for this structure is about 1.2% and 5.7%, respectively. Therefore, the SI of the structure is acceptable. The results of simulation on IR-drop of U-bridge EBG are shown.

ACKNOWLEDGMENT

This work was supported by the Key Lab of High-Speed Circuit Design and EMC, Ministry of Education in China K505120206, and the Fundamental Research Funds for the Central Universities of China JB140220.

REFERENCES

1. Ramesh, A. and V. E. George, "Metallo-dielectric electromagnetic bandgap structures for suppression and isolation of the parallel-plate noise in high-speed circuits," *IEEE Transactions on Microwave Theory and Techniques*, Vol. 51, No. 6, 1629–1639, 2003.
2. Jong, H. K., U. S. Dong, I. K. Sang, and G. Y. Jong, "Novel electromagnetic bandgap array structure on power distribution network for suppressing simultaneous switching noise and minimizing effects on high-speed signals," *IEEE Transaction on Electromagnetic Compatibility*, Vol. 52, No. 2, 365–372, 2010.
3. Wang, T.-K., C.-Y. Hsieh, H.-H. Chuang, and T.-L. Wu, "Design and modeling of a stopband-enhanced EBG structure using ground surface perturbation lattice for power/ground noise suppression," *IEEE Transactions on Microwave Theory and Techniques*, Vol. 57, No. 8, 2047–2054, 2009.
4. Kang, H.-D., H. Kim, S.-G. Kim, and J.-G. Yook, "A localized enhanced power plane topology for wideband suppression of simultaneous switching noise," *IEEE Transactions on Electromagnetic Compatibility*, Vol. 52, No. 2, 373–380, 2010.
5. Ding, T.-H., Y.-S. Li, D.-C. Jiang, Y.-Z. Qu, and X. Yan, "Estimation method for simultaneous switching noise in power delivery network for high-speed digital system design," *Progress In Electromagnetics Research*, Vol. 125, 79–95, 2012.
6. Gao, M.-J., L.-S. Wu, and J. F. Mao, "Compact notched ultra-wideband bandpass filter with improved out-of-band performance using quasi electromagnetic bandgap structure," *Progress In Electromagnetics Research*, Vol. 125, 137–150, 2012.
7. Wu, T.-L., C.-C. Wang, Y.-H. Lin, T.-K. Wang, and G. Chang, "A novel power plane with super-wideband elimination of ground bounce noise on high speed circuits," *IEEE Microwave and Wireless Components Letters*, Vol. 15, No. 3, 174–176, 2005.
8. Wang, X.-H., B.-Z. Wang, Y.-H. Bi, and W. Shao, "A novel uniplanar compact photonic bandgap power plane with ultra-broadband suppression of ground bounce noise," *IEEE Microwave and Wireless Components Letters*, Vol. 16, No. 5, 267–268, 2006.
9. Qin, J. and M. R. Omar, "Ultra-wideband mitigation of simultaneous switching noise using novel planar electromagnetic bandgap structures," *IEEE Microwave and Wireless Components Letters*, Vol. 16, No. 9, 487–489, 2006.
10. Wu, T. L. and T. K. Wang "Embedded power plane with ultra-wide stop-band for simultaneously switching noise on high-speed circuits," *Electronics Letters*, Vol. 42, No. 4, 213–214, 2006.

11. He, Y., L. Li, C. H. Liang, Q. H. Liu, L. Li, and H. B. Wen, "Leafy EBG structures for ultra-wideband SSN suppression in power/ground plane pairs," *Electronics Letters*, Vol. 46, No. 11, 768–769, 2010.
12. He, Y., C.-H. Liang, and Q.-H. Liu, "Novel array EBG structures for ultrawideband simultaneous switching noise suppression," *IEEE Antennas and Wireless Propagation Letters*, Vol. 10, 588–591, 2011.
13. Chu, H., X. Q. Shi, and Y. X. Guo, "Ultra-wideband bandpass filter with a notch band using EBG array etched ground," *Journal of Electromagnetic Waves and Applications*, Vol. 25, Nos. 2–3, 203–209, 2011.
14. He, Y., L. Li, H. Q. Zhai, X. J. Dang, C.-H. Liang, and Q. H. Liu, "Sierpinski space-filling curves and their application in high-speed circuits for ultrawideband SSN suppression," *IEEE Antennas and Wireless Propagation Letters*, Vol. 9, 568–571, 2010.
15. Li, L., Q. Chen, Q.-W. Yuan, and K. Sawaya, "Ultrawideband suppression of ground bounce noise in multilayer PCB using locally embedded planar electromagnetic band-gap structures," *IEEE Antennas and Wireless Propagation Letters*, Vol. 8, 740–743, 2009.
16. Huang, C.-H. and T.-L. Wu, "Analytical design of via lattice for ground planes noise suppression and application on embedded planar EBG structures," *IEEE Transactions on Components, Packaging and Manufacturing Technology*, Vol. 3, No. 1, 21–30, 2013.
17. Wu, T.-L., Y.-H. Lin, and S.-T. Chen, "A novel power planes with low radiation and broadband suppression of ground bounce noise using photonic bandgap structures," *IEEE Microwave and Wireless Components Letters*, Vol. 14, No. 7, 337–339, 2004.
18. Zhang, M.-S., Y.-S. Li, C. Jia, and L.-P. Li, "A power plane with wideband SSN suppression using a multi-via electromagnetic bandgap structure," *IEEE Microwave and Wireless Components Letters*, Vol. 17, No. 4, 307–309, 2007.
19. Kim, B. and D.-W. Kim, "Bandwidth enhancement for SSN suppression using a spiral-shaped power island and a modified EBG structure for a $\lambda/4$ open stub," *Electronics and Telecommunications Research Institute Journal*, Vol. 31, No. 2, 201–208, 2009.
20. Shahparnia, S. and O. M. Ramahi, "Design, implementation, and testing of miniaturized electromagnetic bandgap structures for broadband switching noise mitigation in high-speed PCBs," *IEEE Transactions on Advanced Packaging*, Vol. 30, No. 2, 171–179, 2007.
21. Mahdi, M. S., A. R. Attari, and M. M. Mirsalehi, "Compact and wideband 1-D mushroom-like EBG filters," *Progress In Electromagnetics Research*, Vol. 83, 323–333, 2008.
22. Scogna, A. C., A. Orlandi, and V. Ricchiuti, "Signal and power integrity analysis of differential lines in multilayer printed circuit boards with embedded electromagnetic bandgap structures," *IEEE Transaction on Electromagnetic Compatibility*, Vol. 52, No. 2, 357–364, 2010.
23. He, H.-S., X.-Q. Lai, W.-D. Xu, J.-G. Jiang, M.-X. Zang, Q. Ye, and Q. Wang, "Efficient EMI reduction in multilayer PCB using novel wideband electromagnetic bandgap structures," *International Journal of RF and Microwave Computer-Aided Engineering*, Vol. 21, No. 4, 363–370, 2011.
24. Wu, T.-L., H.-H. Chuang, and T.-K. Wang, "Overview of power integrity solutions on package and PCB: Decoupling and EBG isolation," *IEEE Transactions on Electromagnetic Compatibility*, Vol. 52, No. 2, 346–356, 2010.
25. Pirhadi, A., F. Keshmiri, M. Hakkak, and M. Tayarani, "Analysis and design of dual band high directivity EBG resonator antenna using square loop FSS as superstrate layer," *Progress In Electromagnetics Research*, Vol. 70, 1–20, 2007.
26. Gujral, M. J., L.-W. Li, T. Yuan, and C.-W. Qiu, "Bandwidth improvement of microstrip antenna array using dummy EBG pattern on feedline," *Progress In Electromagnetics Research*, Vol. 127, 79–92, 2012.
27. Kim, S.-H., T. T. Nguyen, and J.-H. Jang, "Reflection characteristics of 1-D EBG ground plane and its application to a planar dipole antenna," *Progress In Electromagnetics Research*, Vol. 120, 51–66, 2011.

28. Kim, K. H. and E. S.-A. José, “Analysis and modeling of hybrid planar-type electromagnetic-bandgap structures and feasibility study on power distribution network applications,” *IEEE Transactions on Microwave Theory and Techniques*, Vol. 56, No. 1, 178–186, 2008.
29. Choi, J., D. G. Kam, D. Chung, K. Srinivasan, V. Govind, J. Kim, and M. Swaminathan, “Near-field and far-field analyses of alternating impedance electromagnetic bandgap (AI-EBG) structure for mixed-signal applications,” *IEEE Transactions on Advanced Packaging*, Vol. 30, No. 2, 180–190, 2007.
30. Raimondo, L., F. D. Paulis, and A. Orlandi, “A simple and efficient design procedure for planar electromagnetic bandgap structures on printed circuit boards,” *IEEE Transactions on Electromagnetic Compatibility*, Vol. 53, No. 2, 482–490, 2011.
31. De Paulis, F., L. Raimondo, and A. Orlandi, “IR-drop analysis and thermal assessment of planar electromagnetic bandgap structures for power integrity applications,” *IEEE Transactions on Advanced Packaging*, Vol. 33, No. 3, 617–622, 2010.
32. Di Febo, D., M. H. Nisanci, F. De Paulis, and A. Orlandi, “Impact of planar electromagnetic band-gap structures on IR-drop and signal integrity in high speed printed circuit boards,” *2012 IEEE EMC ERROPE*, 1–5, Rome, Italy, 2012.